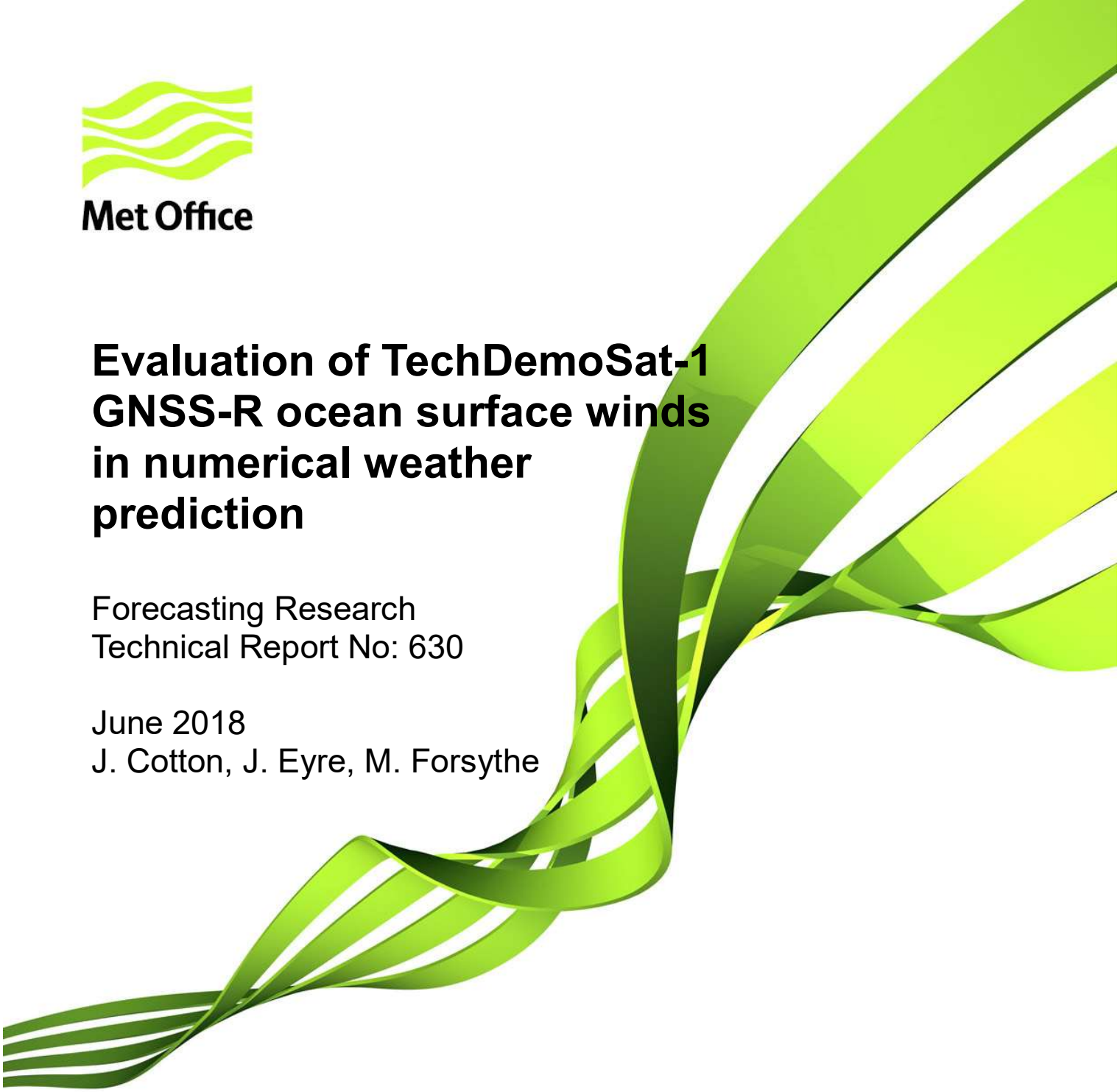

Evaluation of TechDemoSat-1 GNSS-R ocean surface winds in numerical weather prediction

Forecasting Research
Technical Report No: 630

June 2018
J. Cotton, J. Eyre, M. Forsythe

ESA contract TGScatt, 4000116699/16/NL/CT

Abstract

This report was prepared as a contribution to the ESA-funded project, “Scientific assessment of TDS-1 GNSS-R scatterometric measurements” (TGScatt). It summarises the evaluation of ocean-surface wind speeds retrieved from TechDemoSat-1 (TDS-1), within the Met Office numerical weather prediction (NWP) system. TDS-1 wind errors are ~2 m/s but are strongly dependent on the wind speed and this should be taken into account in the observation error assumed in NWP. Spatial averaging in the along-track is beneficial in reducing the noise, especially at higher speeds. For mean wind speed < 12 m/s and 20 observation averaging, the wind speed standard deviation is reduced to 1.78 m/s. Long periods of continuous TDS-1 data collection are needed to evaluate the impact on forecast errors.

1. Introduction

The TechDemoSat-1 (TDS-1) satellite launched on 8 July 2014 is a technology demonstrator mission that carries 8 different payloads, one of which is the Space GNSS Receiver Remote Sensing Instrument (SGR-ReSI) (Unwin et al., 2016). The SGR-ReSI collects reflected signals of opportunity from global navigation satellite system (GNSS) satellites, which have been forward scattered off the Earth surface. The reflected signals contain geophysical information about the reflecting surface and this Earth observation technique is known as GNSS-Reflectometry (GNSS-R) (see Zavorotny, et al., 2014). Over the ocean, GNSS-R roughness measurements have been used for the retrieval of sea surface height, mean square slope (MSS), and ocean surface wind speed.

The ReSI instrument is able to track reflections from up to 4 GNSS satellites simultaneously. The reflected signals are processed on-board the satellite into 2D fields known as delay-Doppler maps (DDMs). Over the ocean, the DDMs show a distinctive horseshoe-shape (Figure 1).

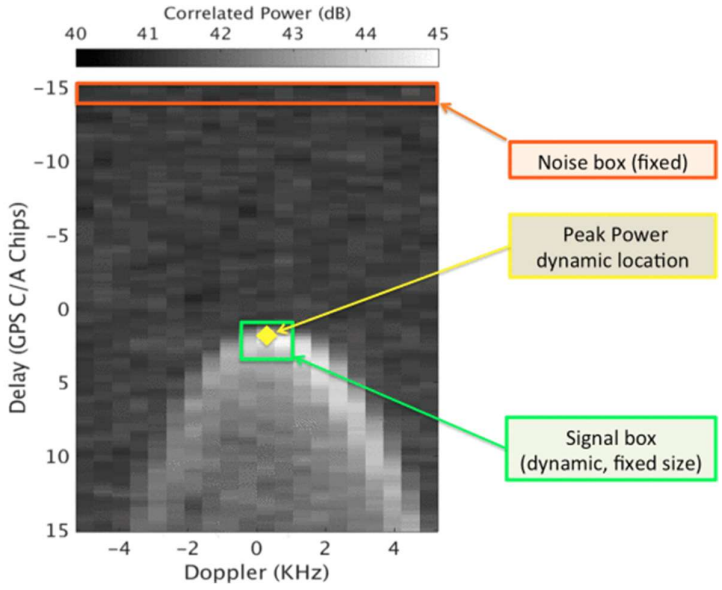

Figure 1. Example of a delay-doppler map (DDM) from TDS-1 acquired over the ocean, showing the DDM areas that can be used to estimate the noise power (orange box), and the signal power (green box) that can be dynamically positioned. Figure reproduced from Foti et al. (2017b).

The retrieval of ocean surface wind speeds from TDS-1 DDMs was first demonstrated by Foti et al., (2015). The retrieval algorithm is based on the signal-to-noise ratio (SNR) and the bistatic radar equation. The antenna received power is estimated from the SNR of:

- the average signal power from a box surrounding the peak of the DDM (size of the signal box determines the spatial resolution),
- the noise power from an area of the DDM with no signal.

A simplified bistatic radar equation (BRE) is used to compute the normalised radar cross-section, σ^0, from the estimated SNR and the bistatic geometry. σ^0 for high SNR cases are then collocated with Advanced SCATterometer (ASCAT) wind speeds to develop a geophysical model function (GMF). Further work by Foti et al. (2017a) allows for radiometric calibration of the observables in the BRE when the receiver is operating in programmed gain mode (CBRE). The importance of using radiometrically calibrated data for the retrieval of geophysical parameters have demonstrated (Foti et al., 2017b).

GNSS-R receivers are low power, low cost and have the potential to increase the temporal and spatial sampling of ocean surface winds through multiple receivers flown in constellation. The NASA Cyclone GNSS (CYGNSS) mission launched in 2016 is a constellation of 8 micro-satellites which carry an upgraded version of the ReSI receiver. Such constellations could complement the existing coverage provided by scatterometers such as ASCAT on Metop. One advantage of GNSS-R is that the L-band signals (~20 cm

wavelength) are less sensitive to precipitation than higher frequencies. A disadvantage is that the signals are not only sensitive to capillary waves driven by the local wind, but also sensitive to other components of the wave field that are less directly related to the local wind.

In this report we evaluate TDS-1 wind speeds within the Met Office numerical weather prediction (NWP) system. TDS-1 winds are based on CBRE version 0.5 winds supplied by the National Oceanography Centre (NOC) and cover the period May-June 2015. A key limitation is the ReSI instrument only operates for 2 days out of every 8, since observation time is shared with other instruments on the platform. This intermittent temporal coverage leaves only a small data set for evaluation. The NOC data have also been pre-filtered to remove retrieved winds greater than 20 m/s (GMF uncertainty at high winds) and data polewards of 55° latitude (sea ice). Note that the imposed 20 m/s cap on the wind speed creates a problem for the subsequent statistical evaluation (see Section 2.2).

A primary tool for evaluating new data sets in NWP is the comparison of the observations (O) to the model background (B) forecast, commonly referred to as O-B. In Section 2 of this report, we define O-B for ocean-surface wind speed observations and summarise the key findings in our assessment of TDS-1.

In Section 3, we consider spatial averaging in the along-track direction in an effort to reduce noise in the measurements.

Because of the sparse temporal availability of TDS-1 data in this study, we use short case studies to help characterise the errors of TDS-1 and its potential impact on NWP. In Section 4, we present several examples comparing TDS-1 with model winds and collocated ASCAT passes. We also demonstrate the wind speed increments applied to the model through a single-cycle assimilation test.

In Section 5, we perform a short impact experiment adding TDS-1 on top of a no-scatterometer winds baseline experiment.

Lastly, our conclusions and recommendations are presented in Section 6.

2. O-B Statistics

Observation minus background (O-B) is the comparison of the observation with the model background state, the short-range forecast that forms the *a-priori* information for the data assimilation.

Global model 6-hour (T+6) forecast fields are retrieved from archive for May and June 2015. At that time, the model had a horizontal grid spacing of ~17 km in the mid latitudes (OS35 configuration). We use an observation operator to forward-model the forecast-equivalent of the observation from the atmospheric state. The model fields are bi-linearly interpolated in space (from the surrounding 4 grid points) and linearly interpolated in time (from T+3, T+6, T+9) to the observation location. The background 10m wind speed is then simply a non-linear function of the 10m zonal and meridional wind components. Note that the O-B contains error contributions from both the observation and the model, and the proper separation of error sources requires additional information, e.g. triple collocation (Lin and Portabella, 2018). However, O-B statistics from other instruments can provide an upper bound for the model error, such that much larger O-B values are likely due to errors in that observation source and not the model.

2.1 2D speed histograms

Considering all data for May and June 2015, TDS-1 wind speed O-B standard deviation (STDV) is around 2 m/s (Figure 2). Considering different latitude bands, STDV values are 2.08 m/s, 1.69 m/s, and 2.39 m/s for the northern hemisphere (NH – polewards of 20°N), tropics (20°N-20°S), and southern hemisphere (SH – polewards of 20°S) respectively. The overall wind speed bias is near zero, but we find a negative bias of 0.4 m/s in the NH statistics (TDS-1 slower than the model). Maps of mean O-B show the source of this difference to be in the North Atlantic (Figure 3).

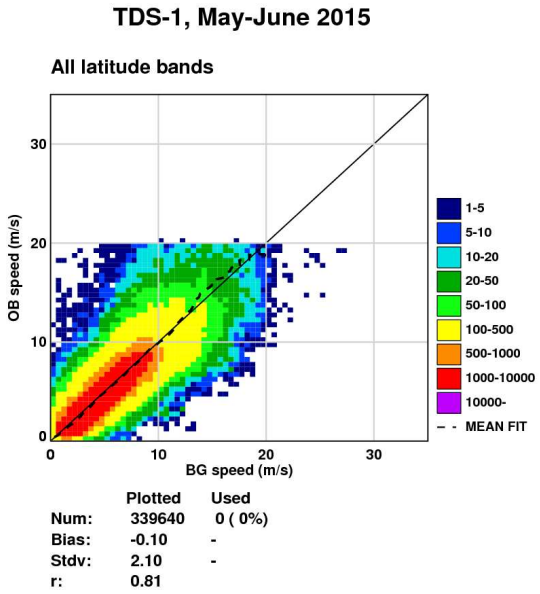

Figure 2. 2-D histogram of TDS-1 wind speed versus the model background wind speed. Data for the period May-June 2015. Note the 20 m/s threshold on the TDS-1 speed.

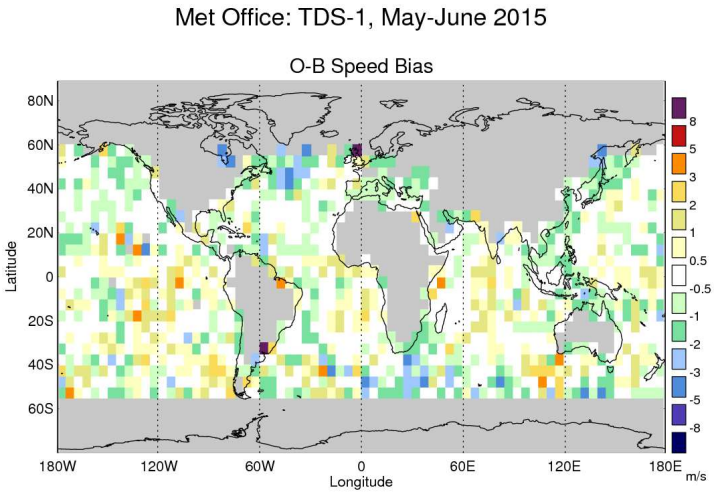

Figure 3. Map of mean O-B speed bias for TDS-1. Data for the period May-June 2015.

2.2 Wind speed dependence

Although STDV is around 2 m/s, the TDS-1 errors are strongly wind speed dependent (Table 1). This can explain the large difference between O-B in the tropics and extra-tropics described in Section 2.1.

In this section statistics are presented in terms of the mean wind speed (MWS), that is the average of the observed and background wind speed

$$MWS = (O + B)/2 \ .$$

STDV values are below 2 m/s for MWS less than 8 m/s, but STDV rapidly increases to 4 m/s for a MWS of 12 m/s (Figure 4, orange line). At higher speeds, there is an artificial decrease in O-B STDV resulting from the 20 m/s upper limit on the TDS-1 retrievals. This effect can be seen by imagining a line perpendicular to the 1:1 line on Figure 2. Considering the mean O-B, absolute wind speed differences are within 0.5 m/s for MWS < 14 m/s.

ASCAT statistics for the same time period show remarkably little increase in STDV with increasing wind speed (Figure 4, green line). ASCAT wind speed STDV is 1.1 m/s overall and in this case remains below 2 m/s for MWS up to 25 m/s. This demonstrates that the large increase in TDS-1 errors with wind speed cannot be due to an increase in the model error, otherwise the same trend would be seen for ASCAT.

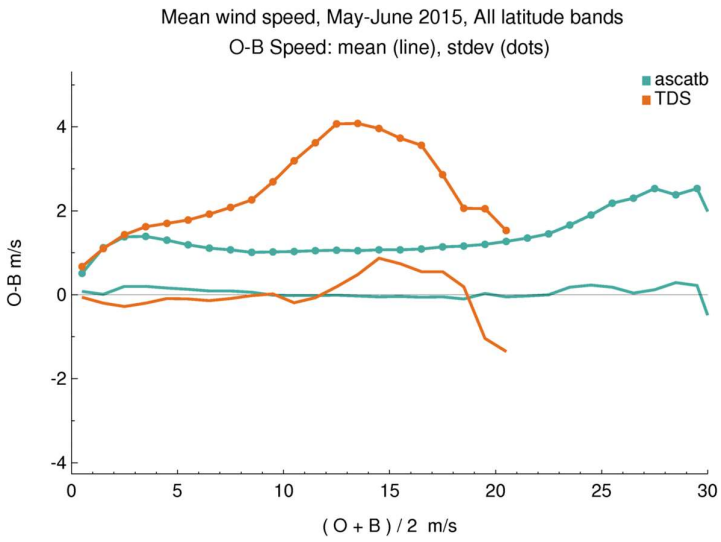

Figure 4. TDS-1 (orange) and ASCAT-B (green) wind speed O-B as a function of the mean wind speed. The mean O-B is shown by solid lines and standard deviation O-B by the line with dot markers. Data plotted are from May and June 2015. ASCAT data have been screened using the wind-vector cell quality flag (KNMIQC including rain, monitor, land, ice) and bias corrected.

	Mean O-B m/s	STDEV O-B m/s	Number
0 ≤ MWS < 4	-0.22	1.40	109,831
4 ≤ MWS < 8	-0.11	1.86	149,184
8 ≤ MWS < 12	-0.05	2.80	63,581
12 ≤ MWS < 16	+0.47	4.01	14,737
16 ≤ MWS < 20	+0.44	3.13	2,288

Table 1. Summary O-B statistics for the TDS-1 data plotted in Figure 4.

2.3 Eclipse flag

Using the supplied eclipse flag we find larger wind speed STDV when the satellite is sunlit (2.20 m/s) compared with in eclipse (1.95 m/s). One factor is the difference in sampling (Figure 5, left) between sunlit/eclipse. In particular, during May/June sunlit data have a much higher sampling of the NH mid-latitudes where STDV is higher. Although the dependence on wind speed is the dominant signal when comparing STDV by latitude, there are clear differences between sunlit and eclipse within the same latitude band (Figure 5, right). Sunlit data have a larger STDV south of the equator, especially 0°-30°S, and eclipse data have a larger STDV north of the equator. This could indicate an issue with the way the sun sensors are used to correct the satellite attitude knowledge. Attitude errors in sunlit parts of the orbit should be smaller than in eclipse where the satellite drifts significantly (Foti et al., 2017b).

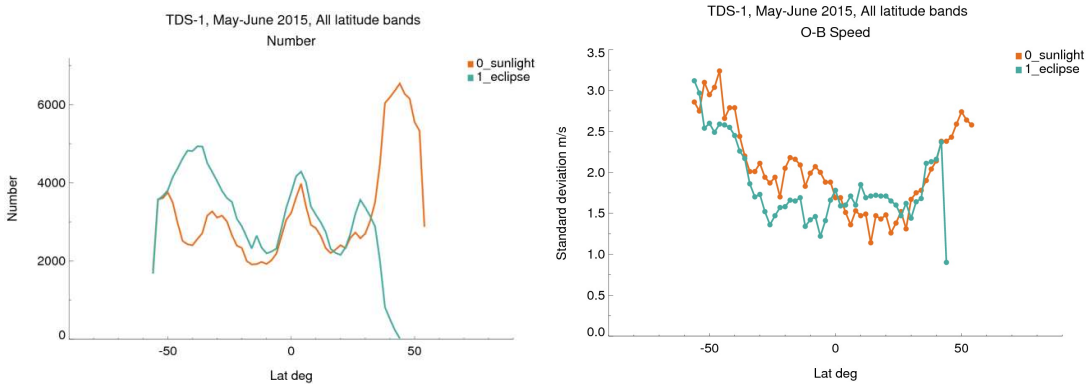

Figure 5. Latitude dependence of the distribution of TDS-1 winds (left), and standard deviation O-B (right). Data are separated by cases when the satellite is sunlit (orange) and in eclipse (green) for the period May-June 2015.

3. Along-track averaging

In an attempt to reduce the noise present in the TDS-1 wind speeds we consider spatial averaging in the along-track direction of the specular point paths. The original data set uses DDMs generated at 1 Hz, giving an along-track separation of around 7 km between winds. Here we consider averaging every 5, 10, or 20 observations, representing a maximum distance between averaged-observations of ~ 28 km, 70 km, or 140 km respectively. As the specular point tracks are non-continuous (fragmented), we add the constraint that there must be a minimum number of winds within the specified maximum

distance in order to form an average. The minimum number of winds are 5, 8, and 16 winds respectively. If the requirement is not met then we shift the averaging window along by 1 observation and try again.

For 5, 10, and 20 observation averaging we reduce the wind speed O-B STDV by 7%, 10%, and 13% respectively. The largest reduction in STDV error (up to around 50%) occurs at higher speeds (Figure 6 b, d). However, note that the STDVs for these data are impacted by the 20 m/s threshold.

If we only consider MWS < 12 m/s, then the reductions in STDV with 5, 10, and 20 observations are 4%, 7%, and 9% respectively. For MWS < 12 m/s and 20 observation averaging, the wind speed STDV is 1.78 m/s.

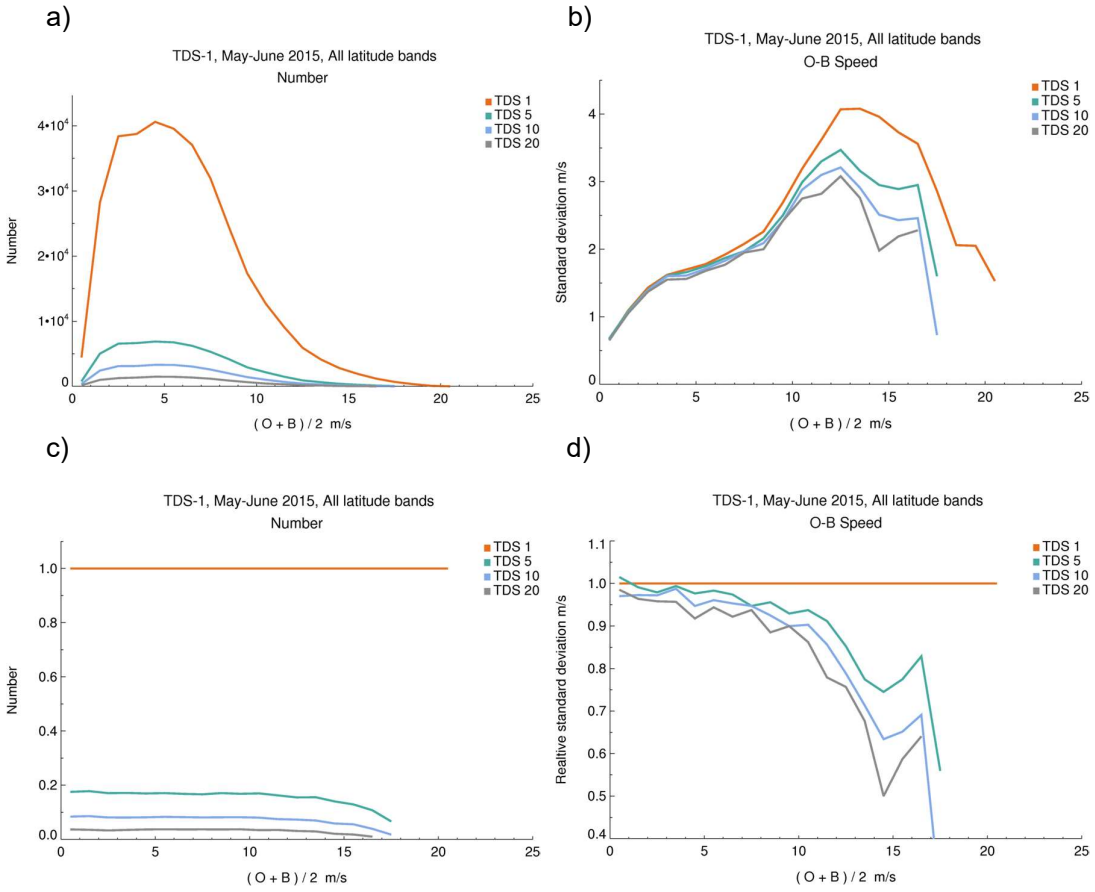

Figure 6. Impact of along-track averaging on the wind speed distribution (a) and standard deviation O-B (b) as a function of the mean wind speed. The orange line shows the original 1 Hz data, and green/blue/grey lines show along-track averaging of 5/10/20 observations. Also shown in (c) and (d) are the same data but normalised by the original 1 Hz values.

4. O-B case studies and single-cycle assimilation test

In this section, we look beyond the statistics and compare TDS-1 with the model and collocated ASCAT passes for individual cases. Selected examples from a 2-day period of continuous data collection between 03/06/2015 1800 UTC – 05/06/2015 1200 UTC are presented below.

i) 03/06/2015 T1800 UTC, west of Australia

West of Australia, two ascending specular point tracks for TDS-1 coincide with an ASCAT pass just 15 mins later (Figure 7 a, b). ASCAT wind speeds reach a minimum at around 26°S, but increase further south. Qualitatively the TDS-1 wind speed track looks similar to ASCAT. We match each TDS-1 wind with the nearest ASCAT wind and compare the wind speed trend along the specular point track. For the left-hand track, we generally find a good agreement in wind speed trend between ASCAT, TDS-1, and the model (Figure 8). There are instances where the data sets differ. At 33.5°S, both ASCAT and the model are 2 m/s faster than TDS-1. At 27.5°S, TDS-1 agrees well with ASCAT, but both are 1-2 m/s faster than the model. Although the overall trend is good, even from this single case it is obvious that TDS-1 noise increases significantly for wind speeds above ~8 m/s.

We test the impact of assimilating the TDS-1 winds by running the data assimilation for a single-cycle. We consider the following cases:

i) Reference
ii) Reference + TDS-1
iii) Reference + ASCAT-A (or ASCAT-B)

In our reference case (i) we assimilate all data (satellite and conventional) apart from the scatterometer winds. We then run the assimilation again and add TDS-1 (ii) or ASCAT (iii) winds and then compare the difference in the analysis increments in each case. In a single-cycle test, we initialise the assimilation from the same background state, ensuring the differences in analysis increment are only due to the different information provided by TDS-1 and ASCAT. Prior to assimilation the data are quality controlled (ASCAT only) and spatial thinning is applied (80 km for both TDS-1 and ASCAT). For this example the assumed ASCAT u/v error is 2 m/s and the assumed wind speed error for TDS-1 is 2 m/s. The different assimilation methods and observation errors are discussed further in the Section 5.

We can identify some similar features in the analysis increments (Figure 7 c, d). Both TDS-1 and ASCAT slow the model analysis wind speed in an area centred near 105°E, 36°S, but the increment is stronger for TDS-1 because it has a larger O-B departure in that area (see Figure 8). If instead we assimilate the 5 observation averaged TDS-1 data, with the same assumed error, then we get smaller increments (not shown). This follows because the averaged data have smaller errors and so we should account for this in the data assimilation.

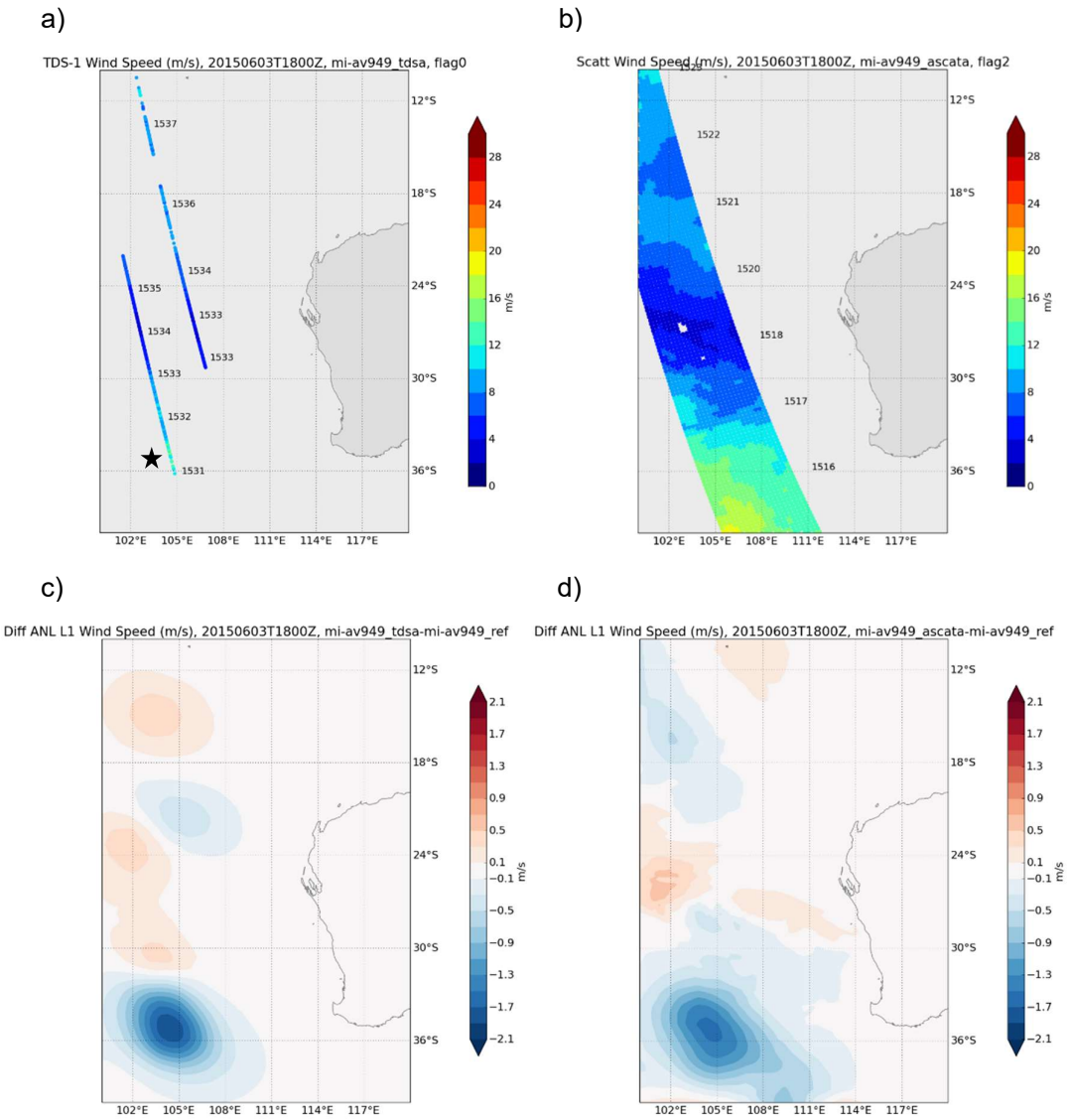

Figure 7. Collocated TDS-1 and ASCAT-A matchup west of Australia for 1800 UTC cycle on 3 June 2015. TDS-1 wind speed (a), ASCAT-A wind speed (b), TDS-1 analysis increment (c), ASCAT-A analysis increment (d). Increments are analysis minus background, where blue (red) shades indicate a slowing (increasing) in wind speed due to the data assimilation. The numbers plotted on (a) and (b) are the observation times in UTC. The star on (a) indicates the track to be collocated with ASCAT in Figure 8.

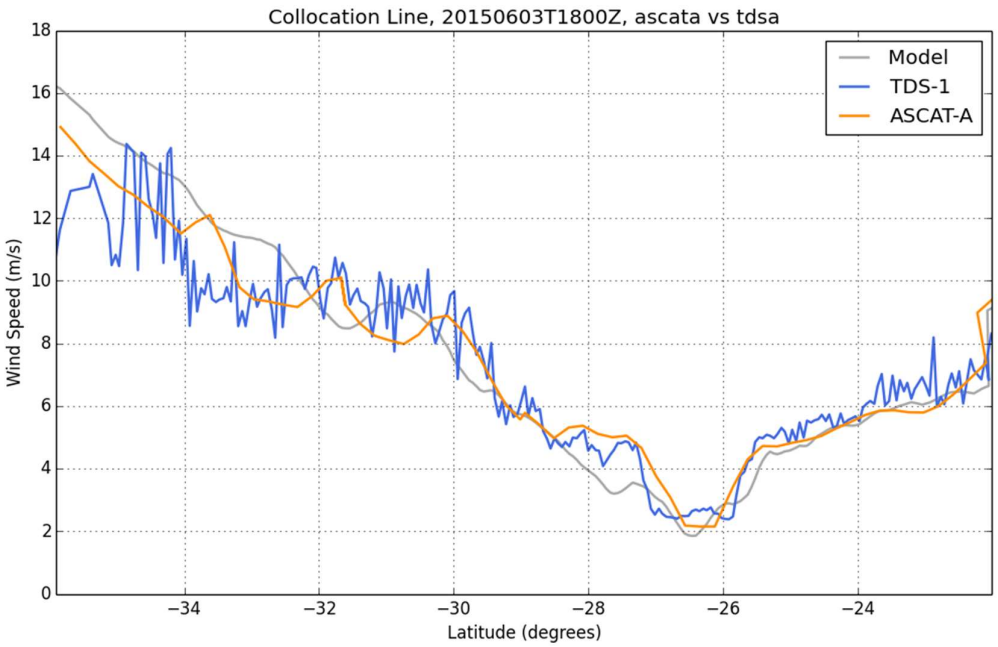

Figure 8. Wind speed trends for collocated TDS-1 (blue line) and ASCAT-A (orange) observations along the western-most specular point track marked with a star in Figure 7a. TDS matched with the nearest ASCAT-A within 50 km. Model winds are at the TDS-1 location. The time difference between passes is 15 mins.

ii) 05/06/2015 T0000 UTC, North Atlantic

In this cycle TDS-1 exhibits a very large negative wind speed O-B in the North Atlantic. Comparing the TDS-1 track with the model background field we find that TDS-1 is completely missing high winds (up to 18 m/s) present in the model near a mid-latitude frontal system (Figure 9 a, b, d). The nearest ASCAT overpass from Metop-B is around 80 mins earlier but this captures well the frontal feature and the strong winds running along it (Figure 9c).

However, further east in the North Atlantic we find a set of TDS-1 tracks to the west of Ireland which intercept a mid-latitude cyclone (Figure 10). In this case TDS-1 is able to capture the trend towards higher wind speed as seen by the model and ASCAT. The coverage near the centre of the storm is limited by the 20 m/s threshold.

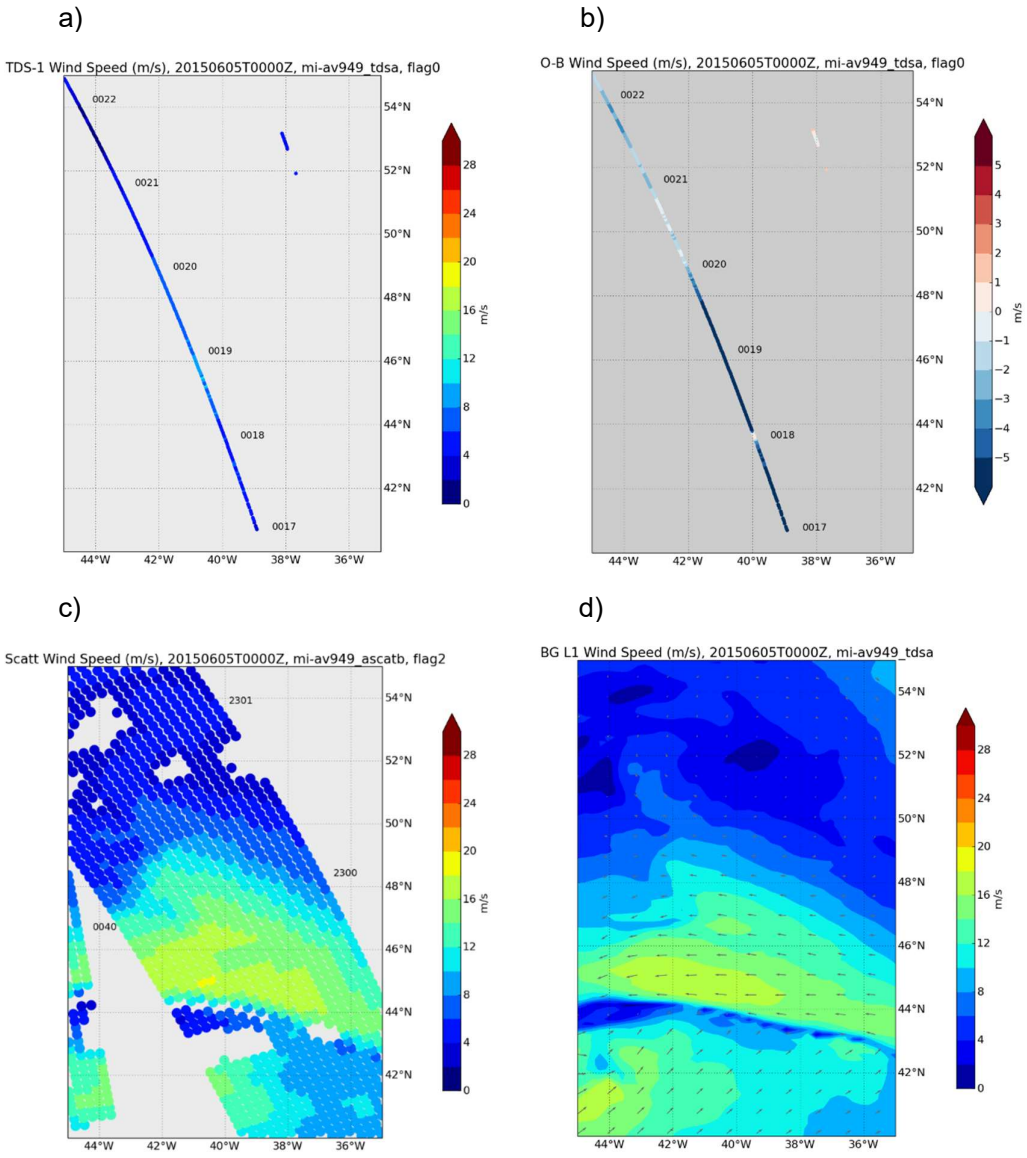

Figure 9. TDS-1 wind speed (a), TDS-1 O-B speed bias (b), ASCAT-B wind speed (c), and 10m model background wind field (d) for 00 UTC cycle on 5 June 2015. The numbers plotted on (a), (b) and (c) are the observation times in UTC. The background field is T+3 forecast valid at 1800 UTC.

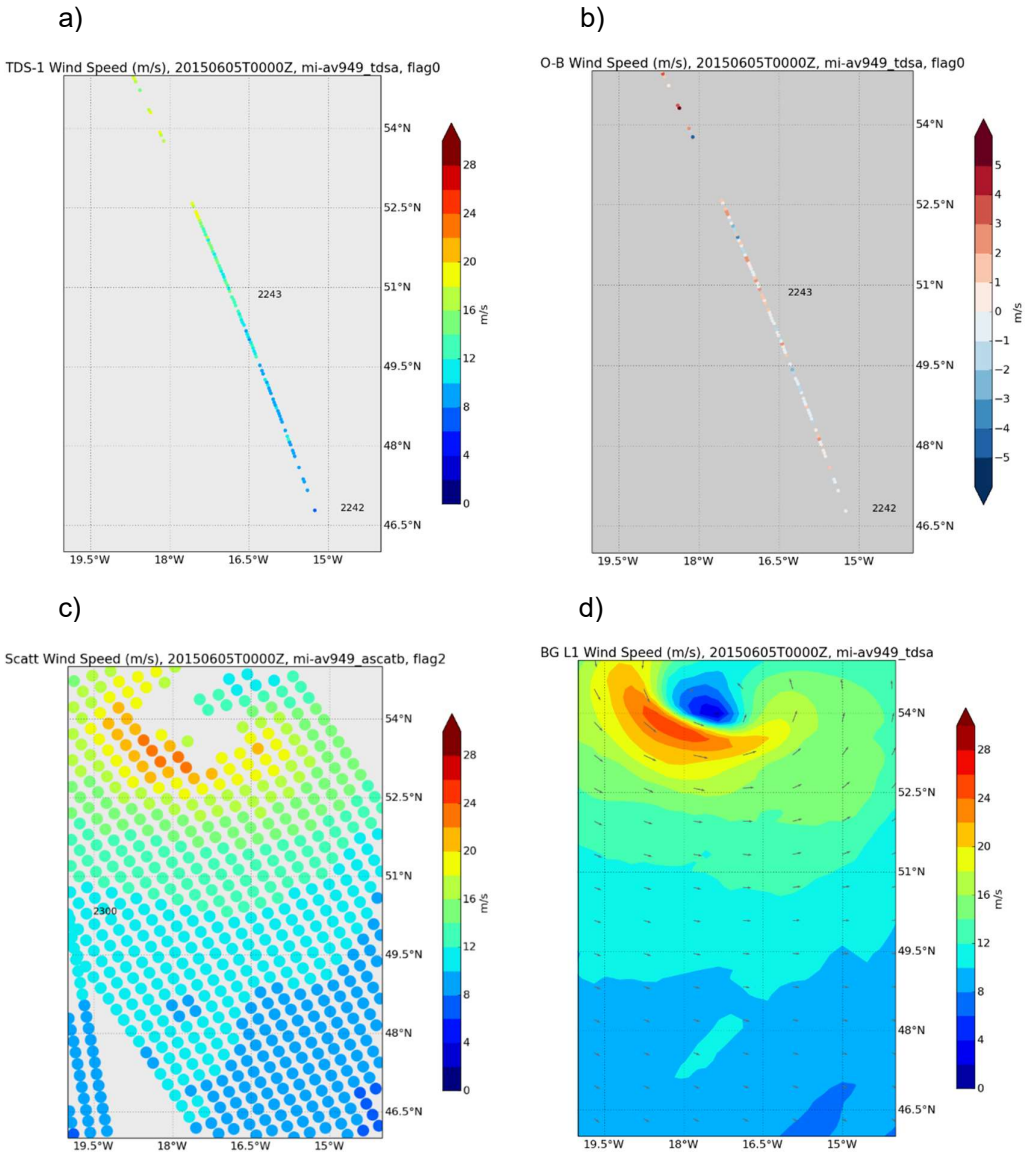

Figure 10. TDS-1 wind speed (a), TDS-1 O-B speed bias (b), ASCAT-B wind speed (c), and 10m model background wind field (d) for 00 UTC cycle on 5 June 2015. The numbers plotted on (a), (b) and (c) are the observation times in UTC. The background field is T+3 forecast valid at 1800 UTC.

iii) 05/06/2015 T1200Z, tropical South Pacific

In the tropics near Vanuatu and New Caledonia, we find TDS-1 has a positive speed bias of several m/s compared to the model and ASCAT (Figure 11).

For each TDS-1 wind we can match with the nearest ASCAT observation and compare the wind speed trend along the western-most specular point track (Figure 12). The ASCAT pass is just 7 mins earlier but passes to the left such that west track of TDS-1 can only be matched with the right edge of the ASCAT swath (Figure 11 a, c). For the track south of

New Caledonia, TDS-1 and ASCAT are in good agreement and around 1 m/s faster than the model. Immediately north of New Caledonia, TDS-1 and ASCAT remain in good agreement and faster than the model, but TDS-1 becomes much noisier with the increase in wind speed. Between 18.5°S and 17°S there is a sudden jump in the TDS-1 wind speed that is not present in either ASCAT or the model, resulting in an O-B up to +9 m/s. Here we consider all TDS-1 data, but a gross-error check could be used as part of the quality control to remove such data with very large O-B departures.

After the spike in wind speed, TDS-1 then remains offset from ASCAT and shows poor agreement with the model trend. In particular, around 14.5°S, 164°E there is a dip in the model wind speed caused by a wind shadow in the lee of an island (see Figure 11d) that is not captured by TDS-1. This could be an error in TDS-1, or model error in overstating the wind shadow. The ASCAT swath is further west of TDS-1 and unable to indicate which is correct.

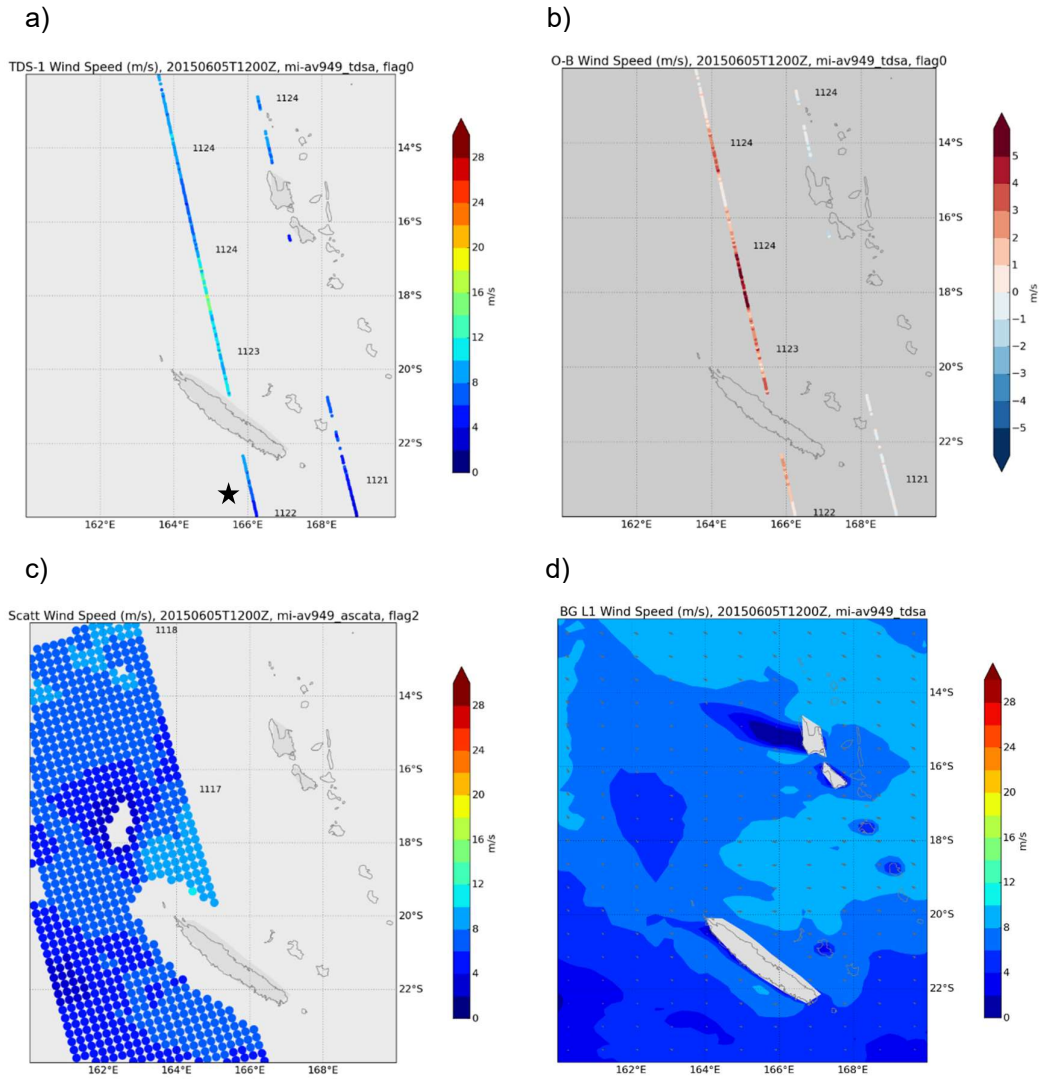

Figure 11. TDS-1 wind speed (a), TDS-1 O-B speed bias (b), ASCAT-A wind speed (c), and 10m model background wind field (d) for 12 UTC cycle on 5 June 2015. The numbers plotted on (a), (b) and (c) are the observation times in UTC. The background field is T+3 forecast valid at 0900 UTC. The large island near the bottom of the image is New Caledonia, the upper-right island chain is Vanuatu. The star on (a) indicates the track to be collocated with ASCAT in Figure 12.

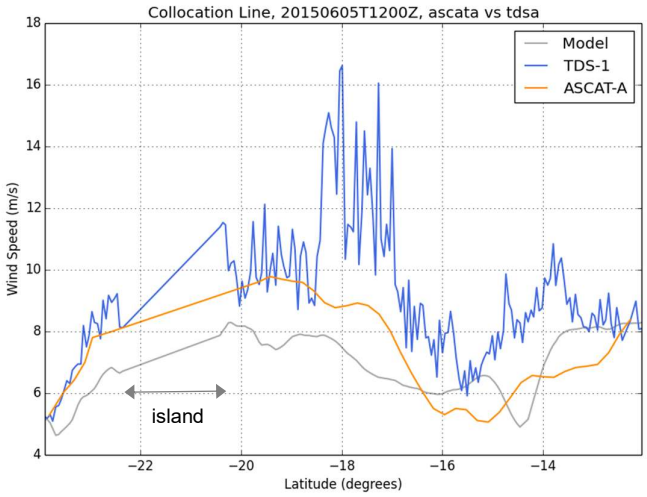

Figure 12. Wind speed trends for collocated TDS-1 (blue line) and ASCAT-A (orange) observations along the western-most specular point track marked with a star in Figure 11a. TDS matched with the nearest ASCAT-A within 100 km. The time difference between passes is 7 mins. The model background wind at the TDS-1 location is plotted in grey.

5. Impact experiment

Observing system experiments (OSEs) usually require several months of data assimilation, ideally across two seasons, to get a reliable signal of impact. With TDS-1 we have data spanning two months but only available for 2 out of every 8 days. Any information gained from TDS-1 in the 2 days available would quickly be lost in the following 6-day data void, washing out any signal.

Instead, we focus on the same 2-day period of continuous data collection from 03/06/2015 1800 UTC – 05/06/2015 1200 UTC and run a short case study experiment. At this time the orbit of TDS-1 is very closely matched to Metop-A/B. The aim of the experiments is therefore to see how much of the impact from ASCAT can be replicated by assimilating TDS-1.

The experiments are defined as follows

- *Reference*: as operations, but no scatterometer winds
- *TDS-1*: Reference + TDS-1 (5 observation averaging)
- *ASCAT-A*: Reference + ASCAT-A
- *ASCAT-B*: Reference + ASCAT-B

For the reference experiment we assimilate all surface-based observations and satellite data that were used in operations at the time, but scatterometer winds are excluded. In the TDS-1 experiment we add the TDS-1 wind speeds on top of the reference. We use the 5 observation averaged TDS-1 data which have smaller errors. In the ASCAT-A and ASCAT-B experiments we add the scatterometer winds from Metop-A/B respectively on top of the reference.

It should be noted the way we assimilate TDS-1 and ASCAT are quite different (Table 2). For TDS-1 we have no quality information provided, but for ASCAT we perform data screening using a quality control (QC) flag, apply SST and wind speed thresholds, and bias correction. Both instruments are thinned in the horizontal to 80 km to mitigate the impacts of correlated error. The biggest difference is that scatterometer winds are assimilated as ambiguous zonal (u) and meridional (v) winds, using information from between 2-4 wind solutions (Cotton, 2013). TDS-1 data are assimilated as wind speeds following the method outlined in Cotton et al. (2018).

The different methods need to be borne in mind when comparing the assumed errors. ASCAT errors are taken to be 2 m/s in u, v (as per operations) but TDS-1 errors are 2 m/s in wind speed (arguably too low for the higher speeds). ASCAT wind speed O-B STDV are about 15-20% smaller than the wind component O-B STDV.

Ideally we would make the assumed observation TDS-1 errors dependent on wind speed, but for this initial experiment we assume them to be constant.

System	ASCAT (as per operations)	TDS-1
Quality control	QC flag, SST threshold, wind speed 2-25 m/s, bias correction	None
Spatial thinning	80 km	80 km
Assumed errors	2 m/s in u/v	2 m/s in wind speed
Assimilation method	Up to 4 ambiguous u/v wind components	Wind speed
Average number assimilated	11,900	480

Table 2. Summary of the assimilation configurations for ASCAT and TDS-1.

For such a short impact experiment we only evaluate the short-range forecast fields. One useful metric is to examine the change in the fit of the background (i.e. the 6-hour forecast) for all the different assimilated observations. The reason for this is that a more accurate analysis should lead to an improved short-range forecast, which should then fit better to the next batch of observations in the next data assimilation cycle (i.e. smaller O-B from an improved B). The benefit of this metric is that because such a large number of satellite observations are assimilated, we can get reliable results even after just a few days.

For the TDS-1 experiment, we find the changes in background fit are neutral.

For the ASCAT-B experiment, we find a reduction of around 1.5% in O-B STDV for Cross-track Infrared Sounder (CrIS) temperature sounding channels in the lower troposphere (Figure 13, bottom). For TDS-1, the O-B STDV for the same CrIS channels are reduced by around 0.5% (Figure 13, top) which, although not statistically significant, demonstrates the change is at least heading in the right direction.

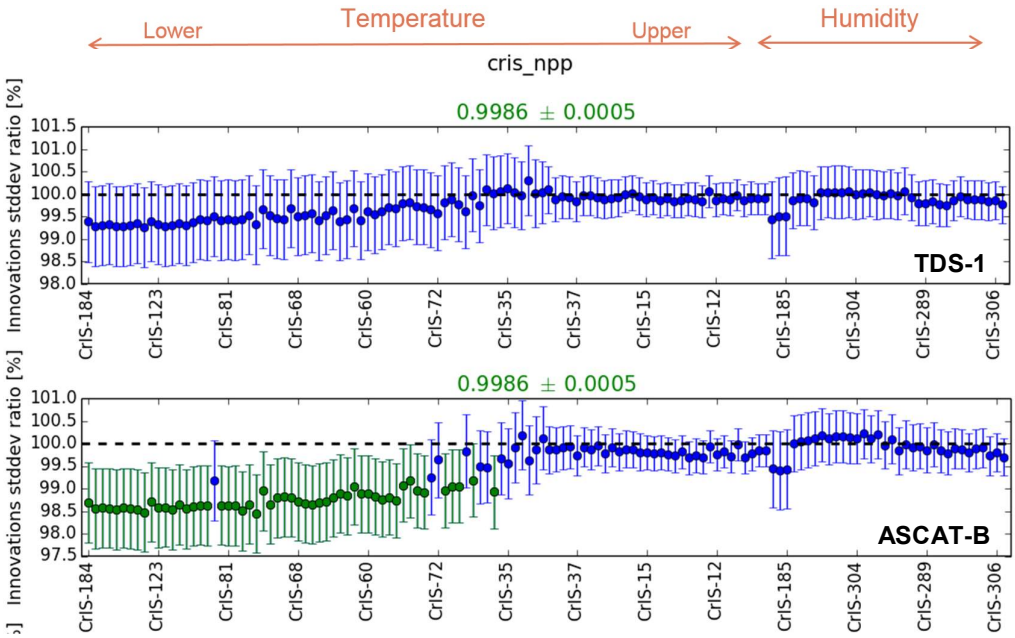

Figure 13. Relative change in standard deviation O-B for CrIS sounding channels on Suomi-NPP. TDS-1 experiment (top) and ASCAT-B experiment (bottom). Changes are relative to a reference experiment with no satellite surface winds. CrIS channels are ordered from left to right in sections, first temperature then humidity sensitive channels. Within these sections, channels are ordered according to the peak of the weighting function in the atmosphere. Blue lines indicate changes that are neutral, green lines indicate reductions in STDV that are statistically significant.

We also compare the change in forecast root mean square error (RMSE) for each of the experiments against independent NWP analyses from ECMWF (Figure 14). Evaluation only considers selected near-surface parameters; pressure at mean sea level (PMSL), 10m winds, and 2m temperatures. Since we only verify ECMWF analyses at 00 UTC and 12 UTC the number of forecast cases is extremely small; four T+6, three T+12, two T+24.

As expected for such a short experiment, the changes in forecast RMSE are not statistically significant for any of the experiments. As such, no firm conclusions about impact can be drawn from these results. Longer scatterometer OSEs demonstrate a beneficial impact on 10m winds (Cotton, 2018) and these short ASCAT experiments are indicative of the same signal. For TDS-1 changes in forecast RMSE are very small.

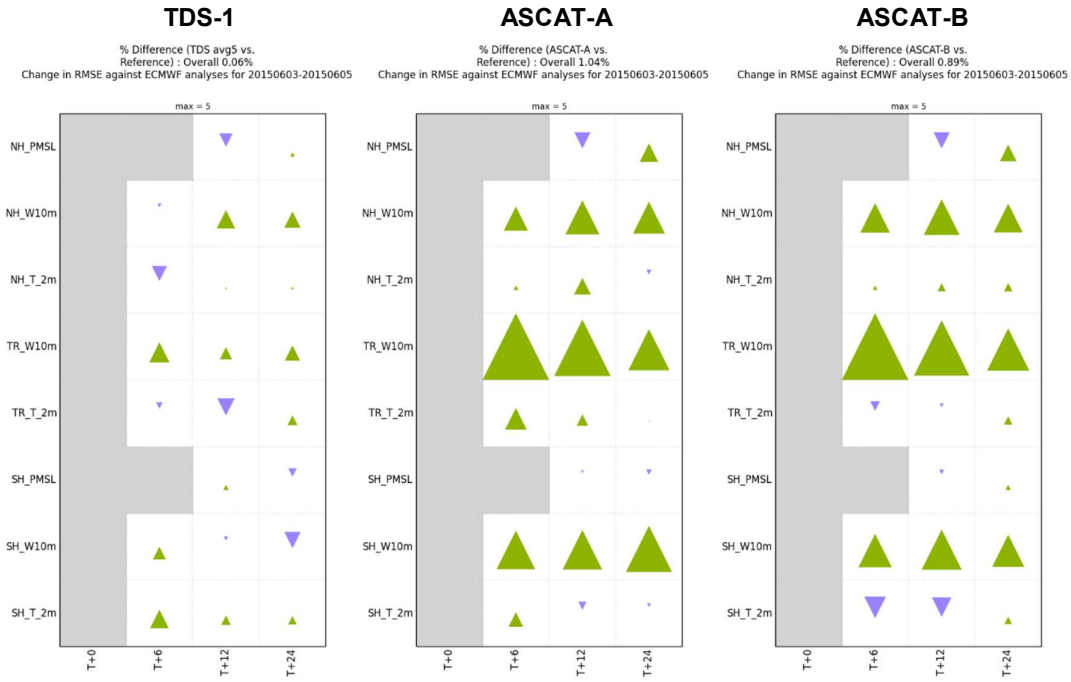

Figure 14. Forecast root mean square error (RMSE) scorecards for the TDS-1 (left), ASCAT-A (middle), and ASCAT-B (right) experiments, versus forecast lead-time. Forecasts are verified against independent ECMWF analyses. The green/upward triangles indicate a positive impact (reduction in RMSE), purple/downward triangles indicate a negative impact (increase in RMSE). Triangles are scaled according to the magnitude of the change in RMSE with a change of 5% entirely filling the box. Forecast parameters are PMSL, 10m winds, and 2m temperatures, in the northern hemisphere (NH), tropics (TR) and southern hemisphere (SH) with boundaries at 20°N/S. None of the RMSE changes are statistically significant at the 95% level.

6. Conclusions and recommendations

TDS-1 wind speed O-B STDV is around 2m/s but the errors are strongly wind speed dependent. Above MWS of 8 m/s, the STDV rapidly increases to a peak of 4 m/s at MWS of 12 m/s. ASCAT statistics for the same time period show remarkably little increase in STDV, remaining below 2 m/s for MWS up to 25 m/s

Spatial averaging in the along-track direction significantly reduces the noise in TDS-1 wind speeds, particularly at higher speeds. For MWS below 12 m/s, the reductions in STDV with 5, 10, and 20 observations averaging are 4%, 7%, and 9% respectively. For MWS < 12 m/s and 20 observation averaging, the wind speed STDV is 1.78 m/s.

Attitude errors in sunlit parts of the orbit should be smaller than in eclipse, but we find STDV is higher for sunlit data south of the equator.

Case studies comparing TDS-1 with the model background and collocated ASCAT passes show examples where:

- Generally good agreement in wind speed trend between ASCAT, TDS-1, and model for a collocation west of Australia. A single-cycle assimilation test show some similarity in the applied analysis increments when we assimilate ASCAT or TDS-1.
- Cases in the North Atlantic show an instance where TDS-1 captures some higher winds associated with a mid-latitude cyclone, but another where TDS-1 completely misses the higher wind speeds seen by ASCAT and the model
- A collocation in the tropical South Pacific shows a large, positive bias (O-B +9 m/s) in TDS-1 wind speed compared to ASCAT and the model.

Since TDS-1 only operates 2 days out of every 8, we limit assimilation experiments to a 2-day period where we have continuous data collection. For the TDS-1 experiment, changes in the fit of the background forecast to other observations are neutral but there are hints the statistics are heading in the right (beneficial) direction. For example, the O-B STDV for the same CrIS channels are reduced by around 0.5% which, although not statistically significant, could indicate TDS-1 is replicating some of the signal we see from ASCAT.

The experiments are too short to draw conclusions on impact on forecast RMSE and longer periods of continuous data observation are required. Since February 2018, TDS-1 has been operating in 24/7 data collection mode and any further impact studies should make use of this new period of data which is planned to continue until the end of 2018.

The impact of observations can depend critically on how the assumed observation errors are modelled. Due to the strong dependence of TDS-1 errors on wind speed, this should be taken into account in order to correctly weight the low and high wind speed. In this study, we have used the close orbit match with ASCAT as a way of evaluating how TDS-1 can replicate the information provided by ASCAT by assimilating the observations independently. Future experiments should consider the ability of TDS-1 to complement the scatterometer winds through the evaluation of TDS-1 impact on top of an ASCAT baseline. Other methods to assess the impact of GNSS-R winds are described in Eyre, 2018.

Here we have considered the TDS-1 winds as being representative of the local wind. However, the MSS measured by GNSS-R is an integral over the whole spectrum and includes components from the (local) wind and (non-local) waves. This wave/swell-excess MSS has largest impact at low wind speeds. Prior information from a wave model could be used to either modify the MSS before the wind retrieval, or as a correction to be applied after wind retrieval using the original MSS.

One of the limitations of the present TDS-1 data set is the pre-screening to restrict data to certain latitude (55° N/S) and wind speed (< 20 m/s) regimes. It would be preferable to instead receive all retrieved winds (excluding those that are obviously erroneous), together with a quality flag that can be used to identify suspect observations. Users can then apply the recommended quality screening or develop their own method.

Acknowledgements

Thanks to John Eyre and Mary Forsythe for their helpful comments in preparing this report.

References

Cotton, J. (2013). Assimilating Scatterometer Winds from Oceansat-2: Impact on Met Office Analyses and Forecasts. Forecasting Research Technical Report No. 572,

February 2013. Available from https://www.metoffice.gov.uk/learning/library/publications/science/weather-science-technical-reports.

Cotton, J. (2018). Update on surface wind activities at the Met Office. Proceedings of the 14th International Winds Workshop, Jeju, South Korea, 23-27 April 2018. Available from http://cimss.ssec.wisc.edu/iwwg/iwwg_meetings.html.

Cotton J., Francis, P., Heming, J., Forsythe, M., Reul, N., Donlon, C. (2018). Assimilation of SMOS L-band wind speeds: impact on Met Office global NWP and tropical cyclone predictions. Q.J.R. Meteorol. Soc., **144** (711), 614-629, doi:10.1002/qj.3237.

Eyre, J. (2018). Observing system studies proposed for GNSS-R ocean surface wind data. . Forecasting Research Technical Report No. 629, June 2018. Available from https://www.metoffice.gov.uk/learning/library/publications/science/weather-science-technical-reports.

Foti, G., Gommenginger, C., Jales, P., Unwin, M., Shaw, A., Robertson, C, Rosello, J. (2015). Spaceborne GNSS reflectometry for ocean winds: First results from the UK TechDemoSat-1 mission. *Geophysical Research Letters*, **42** (13), 5435-5441, doi: 10.1002/2015GL064204.

Foti, G., Gommenginger, C., Srokosz, M. (2017a). First spaceborne GNSS-Reflectometry observations of hurricanes from the UK TechDemoSat-1 mission. *Geophysical Research Letters*, **44**, 12358–12366, doi: 10.1002/2017GL076166.

Foti, G., Gommenginger, C., Unwin, M., Jales, P., Tye, J., Roselló, J., (2017b). An Assessment of Non-geophysical Effects in Spaceborne GNSS Reflectometry Data From the UK TechDemoSat-1 Mission. *IEEE Journal of Selected Topics in Applied Earth Observations and Remote Sensing*, **10** (7), 3418-3429, doi: 10.1109/JSTARS.2017.2674305.

Lin, W., Portabella, M. (2018). Consolidation and validation of Level 1 to Level 2 inversion algorithms. TGSCATT project technical note TN5.

Unwin, M., Jales, P., Tye, J., Gommenginger, C., Foti, G., Rosello, J. (2016). Spaceborne GNSS-reflectometry on TechDemoSat-1: Early mission operations and exploitation. *IEEE Journal of Selected Topics in Applied Earth Observation and Remote Sensing*, **9** (10), 4525-4539, doi: 10.1109/JSTARS.2016.2603846.

Zavorotny, V., Gleason, S., Cardellach, E., Camps, A. (2014). Tutorial on remote sensing using GNSS bistatic radar of opportunity. *IEEE Geosci. and Remote Sensing Magazine*, **2** (4), 8-45, doi: 10.1109/MGRS.2014.2374220.